JOURNAL OF CATALYSIS **79**, 431–444 (1983)

The Interaction of Acetaldehyde and Acetic Acid with the ZnO Surface

M. BOWKER, H. HOUGHTON, AND K. C. WAUGH

ICI Corporate Laboratory, P.O. Box 11, The Heath, Runcorn, Cheshire, WA 7 4QE, United Kingdom

Received May 26, 1982; revised October 15, 1982

The adsorption and reaction of acetaldehyde and acetic acid with defected zinc oxide was studied using the technique of temperature-programmed reaction (TPR). The observed interaction with the surface is analogous with the reactions reported previously for the corresponding monocarbon molecules (M. Bowker, H. Houghton, and K. C. Waugh, *J. Chem. Soc. Faraday I* **77**, 3023 (1981)). Thus acetaldehyde undergoes nucleophilic attack by surface oxygen to produce a very strongly bound species, namely, the acetate. Similarly, acetic acid adsorbs to produce the same acetate moiety by deprotonation. Upon temperature programming some of the parent molecules are liberated into the gas phase just above room temperature, and then the acetate is observed to decompose at approximately 600K. The products of decomposition are acetic acid, ketene, CO_2, H_2, and H_2O; after this desorption, hydrogenated carbidic remnants are left on the surface which react with surface oxygen and liberate CO and H_2 into the gas phase at 700K. In addition to these products acetaldehyde adsorption results in the formation of an ethoxy intermediate which decomposes at 530K in a characteristic fashion to produce ethylene and hydrogen, with the oxygen abstracted by the surface.

INTRODUCTION

In previous papers (*1*, *2*) the adsorption of CO, CO_2, H_2, and several simple organic molecules (methanol, ethanol, methyl formate, and formaldehyde) on the defected zinc oxide surface was reported. The behavior of methanol contrasted markedly with that of ethanol in that the former was observed not only to dehydrogenate, but also to suffer nucleophilic attack by surface oxygen species resulting in the formation of a strongly bound formate moiety (*1*); no comparable species, like the acetate, for instance, was seen with the latter, the molecule being dehydrated to yield ethylene and hydrogen in the gas phase and reincorporate oxygen into the surface (*2*). It was inferred that this difference was due to the geometry of adsorbed ethanol which enables the methyl group to interact with oxygen atoms in the surface, while bonding to the surface primarily through the oxygen atom of the molecule, this latter bonding mode having been identified for alcohols on metal surfaces (*3*). Like methanol, formaldehyde undergoes nucleophilic attack on the surface to produce the formate entity, although considerable amounts of methanol were produced by hydrogenation of formaldehyde to produce the methoxy species and thence methanol by further hydrogenation (*1*). Methyl formate also underwent nucleophilic attack to produce formate and methoxy species; as a result both methanol and formaldehyde were evolved in addition to the CO and hydrogen evolution from formate decomposition (*2*).

In the present study the earlier work has been extended to include the C_2 analogs of formaldehyde and methanol, viz., acetaldehyde and acetic acid, as a means of gaining an increased understanding of mechanistic pathways on oxide surfaces.

A considerable amount of work has now been presented by Madix and coworkers (*3*) on the reaction of such molecules with well-defined metal surfaces; the reactions with copper and silver surfaces are of particular interest, since the heat of adsorption is low enough to avoid complete rupture of the molecules, the latter mode of reaction

0021-9517/83/020431-14$03.00/0

being seen on metals with only partially filled *d*-bands such as W(*5*), for example. Reaction occurs with the dissociation of the most weakly bound hydrogen atoms first, and these are attached to the oxygen atoms in the molecule (since such species adsorb via the oxygen end of the molecule (*4, 6*), the O–H bond is weakened). Thus, for instance, stable intermediates observed on copper surfaces are alkoxys and carboxylates (by deprotonation of alcohols (*4*) and acids (*5–7*)), while aldehydes, ketones, and esters require the presence of oxygen on the surface in order to react. Aldehydes react with chemisorbed oxygen atoms to produce carboxylates (*6, 7*). All these species further decompose above room temperature to yield dehydrogenated products into the gas phase.

Less work has been carried out under well-defined conditions to investigate the reactivity of such molecules with oxide surfaces. Parrott *et al.* (*8*) reported the reactions of ethanol, propanol, and acetic acid with the surface of MgO, using temperature-programmed desorption, the technique also used in this work; the major products were found to be dehydrated, that is, ethylene, propylene, and ketene.

The investigation technique used in this and the previous work is that of temperature-programmed desorption, a method pioneered in well-defined surface reaction studies mainly by Madix (*3*). Due to readsorption phenomena within finely divided catalytic samples (as opposed to single-pass, single-crystal experiments) desorption curve lineshapes are broadened resulting in the inapplicability of lineshape analysis methods (*9*). However, peak temperatures give a reasonable estimate of relative kinetics for processes taking place in different temperature regimes and in this work solution of Eq. (A) was used to elucidate approximate activation energy barriers to surface reaction processes:

$$E_d/RT_p^2 = \nu/\beta \exp(-E_d/RT_p), \qquad \text{(A)}$$

where E_d is the activation energy barrier for a first-order desorption or decomposition process, R is the Boltzmann constant, T_p is the experimental temperature of the peak rate, ν is the frequency factor, and β is the heating rate. ν is assumed to be of normal vibrational frequency dimensions, that is, 10^{13} s^{-1}. The derived E_d values are therefore only representative of the relative rates of the surface kinetic processes.

EXPERIMENTAL

The equipment used has been described in detail previously (*1*). The temperature-programmed desorption and reaction experiments were all carried out at a heating rate of 0.7K s^{-1}, and all products were monitored on a Vacuum Generators Model QX200 quadrupole mass spectrometer. However, the heating rate is nonlinear in the low-temperature region up to 400K; the heating rate profile is shown in Fig. 1. Blank experiments showed that the contribution to the desorption signal from material adsorbed on the filament was negligible due to its low surface area (approximately 0.005% of the ZnO area).

The ZnO sample was Analar (99.7% pure) and the major impurity is quoted as carbonate, at a level of 0.25%. The surface area of the sample was determined to be 3 m^2 g^{-1} by the BET method. The Analar sample was fairly well defined consisting of crystallites of typical length ~3000 and 1000 Å in diameter.

The gases used in this study were liquids at room temperature and were purified by cycles of freezing, thawing, and pumping. The absorbate was dosed through a needle valve from the equilibrium vapor pressure above the liquid in a closed dosing line. Vapor purity could be checked by (i) constancy of the pressure above the liquid and (ii) analysis of the mass spectral cracking pattern in the adsorption system. Both adsorbates were dosed from an ambient partial pressure of ~10 Torr for 15 min at 320K, after which the gas supply was closed off and the system was pumped

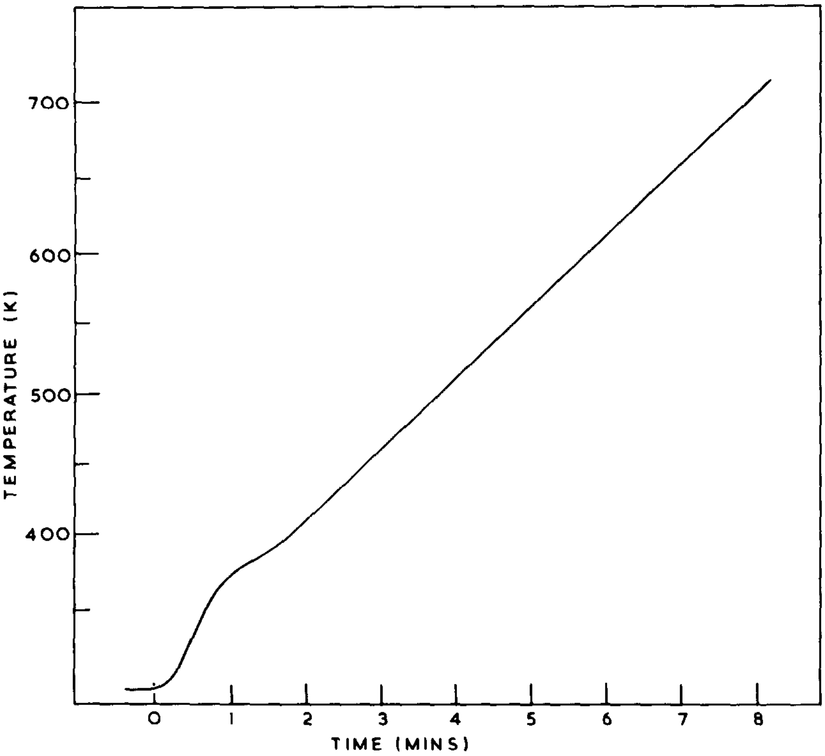

FIG. 1. Heating rate profile for the temperature-programmed desorption experiments on ZnO.

down to 10^{-7} Torr before temperature programming was initiated.

RESULTS AND DISCUSSION

First Heating

The desorption of material upon first heating the zinc oxide sample was the same as that reported in Ref. (*1*). Mainly CO_2 and water were desorbed and are thought to arise from the decomposition of carbonate and hydroxyl species in the sample. After this first heating (taken up to a temperature of 700K) further thermal treatment showed negligible desorption of gases.

As described in the preceding paper the ZnO surface was found to be much more active to adsorption when pretreated in hydrogen at elevated temperatures. Hence, in this study, the sample was prereduced in ~10 Torr of hydrogen for 15 min at 530K prior to exposure to the adsorbate of interest.

The Adsorption of Acetic Acid

The desorption products observed after the adsorption and reaction of acetic acid with the defected ZnO surface at 320K are shown in Fig. 2. The major desorption features are the evolution of acetic acid, hydrogen, and water just above room temperature followed by a complex product spectrum peaking at ~600K with CO and hydrogen finally evolving coincidently at 690K. The intermediates responsible for the latter desorption are the most stable yet observed on this zinc oxide sample in this series of studies.

The major products evolving at 600K are acetic acid (CH_3COOH), ketene (CH_2CO), CO_2, H_2, and H_2O. Acetic acid is "fingerprinted" by large signals at m/e 43, 45, and 15, while large peaks of m/e 14 and 42 are indicative of ketene. The assignment of desorption products has been discussed in detail in other works (*7*, *15*).

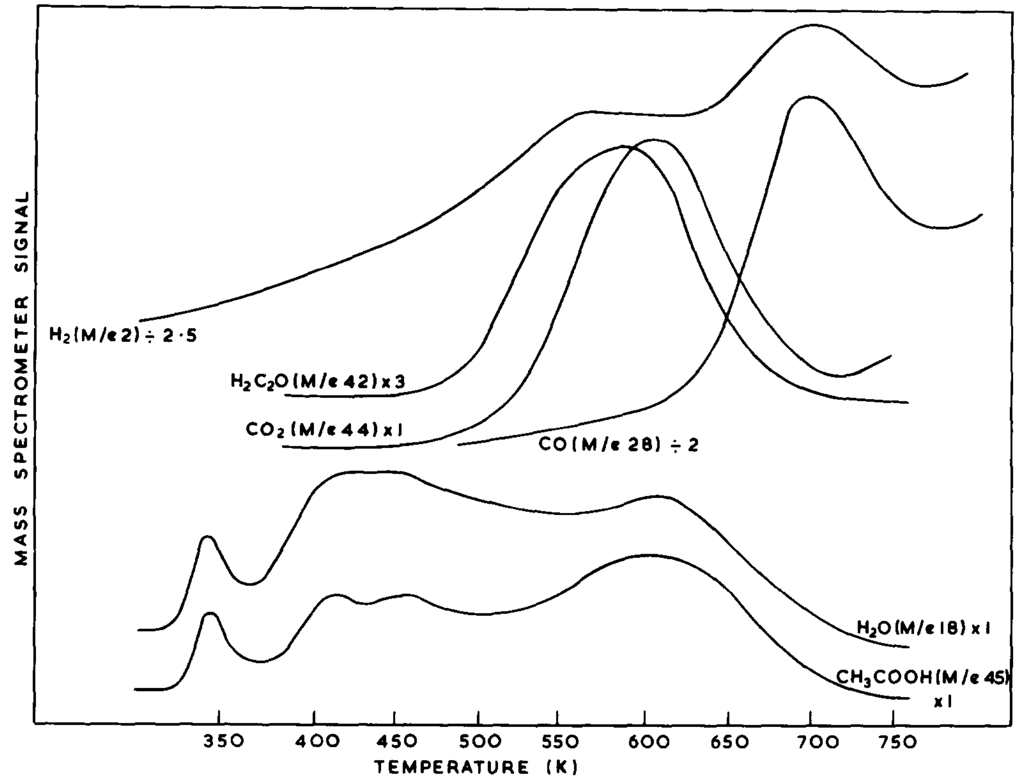

FIG. 2. Temperature-programmed desorption spectrum of products observed after dosing the ZnO sample with acetic acid at 320K. The curves for different products are offset vertically for clarity.

The total amount of acetic acid which adsorbed was measured from the integral of the desorption curves for every mass peak, knowing the pumping speed of the system (1 liter s^{-1} for N_2) and mass spectrometer sensitivity for each product (*10*). The total coverage is given in Table 1, together with the coverages of the various intermediates observed in the desorption spectra. The total coverage is around half of a monolayer (where a monolayer is defined as equal the number of surface layer atoms—for the polar face of ZnO, for instance, this value is 1.1×10^{15} Zn atoms cm^{-2}).

The thermal desorption technique is a dynamic method, observation of reaction mechanisms being generally made well away from equilibrium, since gas evolved during desorption is rapidly removed by pumping. Single steps within a global reaction mechanism can be separated out into various temperature regimes and reaction mechanisms can therefore be defined with some certainty. The following mechanistic route for the adsorption and reaction of acetic acid with the zinc oxide surface accounts for the products seen in the desorption spectra.

The first step in the process is acetic acid adsorption on the surface,

$$CH_3COOH_{(g)} \rightarrow CH_3COOH_{(a)}, \quad (1)$$

where the subscripts (g) and (a) represent gas phase and adsorbed species, respectively. Adsorption of simple organic molecules on metal surfaces has been shown by spectroscopic methods (including XPS and UPS) to occur generally through interaction of the oxygen atoms of the molecule with the surface (*4, 6, 11, 12*). In particular, acetic acid adsorbs on copper surfaces in this manner (*16*). Other work on zinc oxide

TABLE 1

Surface Coverages by Acetic Acid and Acetaldehyde

Adsorbate	Total amount adsorbed[a] (molecules $cm^{-2} \times 10^{-14}$)	Adsorbed intermediates	Coverage intermediate (molecules $cm^{-2} \times 10^{-14}$)	Desorption products/ temperature of peak desorptions	Amount of product desorbed (molecules $cm^{-2} \times 10^{-14}$)
CH_3COOH	6.4	CH_3COO (stable up to ~580K)	6.4	CH_3COOH/<500K	~1.7[c]
				H_2O/<500K	~0.6[c]
				CH_2CO/585K	~0.9
			4.7	CH_3COOH/610K	~2.6[c]
				CO_2/610K	1.3
				H_2O/610K	0.5
				H_2/~580K	~0.3
				CO/690K	1.1
		CH_x (produced after acetate decomposition)	1.1+[b]	H_2/690K	0.45
CH_3CHO	2.5	CH_3CHO	1.3	CH_3CHO/<450K	1.3
				H_2O/<450K	~0.2
		CH_3CH_2O	0.3	C_2H_4/535K	0.3
				H_2 or H_2O/535K	
		CH_3COO	0.9	H_2/610K	0.7
				CH_2CO/615K	0.2
				CO_2/635K	0.3
				CH_3COOH/635K	0.4
		CH_x	0.3+[b]	CO/685K	0.3
				H_2/~670K	~0.1

[a] Estimated uncertainty in absolute values of coverage is 30% from the reproducibility of peak integrals.

[b] Small amounts of C are left on the surface after decomposition of this intermediate species.

[c] Deconvolution of the peaks into high-temperature and low-temperature peaks is not certain, though the total acetic acid desorbed is full integral between 350 and 750K of the curve in Fig. 1.

surfaces has shown a similar bonding mode for molecules such as methanol (*13, 14*), formaldehyde (*12*), and ethylene oxide (*14*). Such bonding will result in a weakening of the O–H linkage in acetic acid and thus, being now the weakest bond, renders it liable to complete rupture. This was shown to be the case on copper surfaces (*7*) and the species formed by this reaction was the acetate, with the two oxygen atoms being bonded with the surface in identical configurations. In the present case, however, oxygen atoms are present on the surface and so dissociation probably occurs by an acid–base type of reaction resulting in hydroxyl formation,

$$CH_3COOH_{(a)} + O_{(s)} \rightarrow CH_3COO_{(a)} + OH_{(a)}, \tag{2}$$

where $O_{(s)}$ represents a lattice oxygen atom. This step could occur in two possible ways: (i) by a simple acid–base reaction as stated above or (ii) by nucleophilic attack at the acid group carbon atom by the surface oxygen. The latter is mentioned since methyl formate was observed to react by that route as shown above—resulting in formate formation by the splitting off of the methoxy group (*2*). Such a reaction is extremely unlikely in this case since the acetic acid contains a hydrogen atom which is much more "acidic" than any in methyl formate. Furthermore, experiments carried out by Barteau *et al.* (*15*), using labeled oxygen predosed onto a silver surface, showed that $H_2{}^{18}O$ was produced and none of the acetates produced contained any labeling. Soon after heating is initiated water is evolved, as is acetic acid. The water may be evolved by two possible processes, depending on the state of the adsorbed acetic acid species. The desorption pattern shows two completely different forms of acetic acid—the form which results in the low-temperature desorption and the form yielding products above 550K. However, the state of the species leading to the low-temperature desorption is uncertain—it may be a molecularly adsorbed entity or dissociated. If it is dissociated then recombination with OH groups, or possibly adsorbed hydrogen atoms, results in the formation of adsorbed acetic acid,

$$CH_3COO_{(a)} + OH_{(a)} \rightarrow CH_3COOH_{(a)} + O_{(s)}, \quad (3a)$$

$$CH_3COO_{(a)} + H_{(a)} \rightarrow CH_3COOH_{(a)}, \quad (3b)$$

and water production may occur by either of the following processes:

$$2OH_{(a)} \rightarrow H_2O_{(g)} + O_s, \quad (4a)$$

$$CH_3COOH_{(a)} + OH_{(a)} \rightarrow CH_3COO_{(a)} + H_2O_{(a)}, \quad (4b)$$

$$CH_3COOH_{(a)} \rightarrow CH_3COOH_{(g)}, \quad (5)$$

$$H_2O_{(a)} \rightarrow H_2O_{(g)}. \quad (6)$$

As can be seen from Table 1, most of this water (or hydrogen) is lost from the surface upon adsorption, since the amount of hydrogen evolved in the low-temperature peaks is only one-fourth of the acetic acid which is left dissociated on the surface above 500K. Some hydrogen and carbon monoxide was seen to evolve coincidently with the low-temperature acetic acid and water but, as pointed out for the other molecules in a previous paper (*2*), blank experiments with acetic acid in the gas phase at a pressure of $\sim 5 \times 10^{-6}$ Torr showed that these products were the result of cracking of acetic acid at the hot Pt–Rh heating filament. Such products were only seen as peaks at the low temperature because of the rapid heating and cooling of the filament at the low end of the temperature regime as the programmer seeks to establish linearity.

After the low-temperature desorption, above approximately 500K, the major species left on the surface has the stoichiometry of the acetate, $CH_3COO_{(a)}$. This species then cannot desorb intact and instead decomposes to other neutral gas-phase products above 550K. The major products are outlined above and in Table 1 and are very similar to those seen for acetate groups adsorbed on copper (*7*) and silver (*15*) surfaces. The only major difference is that large amounts of methane were observed to be produced from this process on the metal surfaces, whereas none was seen here (this point is discussed further below). The evolution of acetic acid and ketene from the acetate decomposition indicates some intermolecular rearrangement on the surface and participation of a further intermediate in this complex reaction is inferred, that is, the acetic anhydride intermediate. Blake and Speis (*16*) have reported results for the decomposition of acetic anhydride in the gas phase and the decomposition products are ketene and acetic acid. The anhydride must be formed by interaction between two acetate moieties and is represented by

$$2CH_3COO_{(a)} \rightarrow (CH_3CO)_2O_{(a)} + O_{(s)}. \quad (7)$$

There are several reasons to believe that this is indeed the species responsible for the production of acetic acid and ketene. The involvement of anhydride in acetic acid decomposition on copper (*7*) and silver (*15*) surfaces has been invoked. A long-lived acetic anhydride form was postulated by Madix *et al.* (*17*) on a single-crystal Ni(110) surface at 300K, water being eliminated into the gas phase upon adsorption of acetic acid and consequently anhydride formed. X-Ray photoelectron spectroscopy results by Kishi and Ikeda (*18*) suggest the presence of both acetate and acetyl (CH_3CO) groups on polycrystalline iron and nickel surfaces, and these two species are combined in the anhydride (though they found no distinct evidence for the latter). These findings support the proposition of mechanistic step (7) and the acetic anhydride intermediate. However, whether it is a stable intermediate present below 600K on the ZnO surface (as on the Ni surfaces described above) or whether it exists simply as a transition state between acetate groups and gas-phase products and as such is very short-lived (as appears to be the case on copper (*7*) and silver surfaces (*15*) since no direct evidence for its existence in a stable form was found by XPS) has not been determined; an answer to this question requires further study using surface spectroscopic techniques (such as X-ray photoelectron spectroscopy) not available on the equipment used in this work.

An alternative model for decomposition would have to involve two separate mechanisms, one involving acetate decomposition to ketene by β-C hydrogen removal (as proposed in the previous paper for ethoxy decomposition to ethylene (*2*)) and subsequent deoxidation. The other involves acetate decomposition to give adsorbed carbonaceous groups and CO_2 liberation into the gas phase. The anhydride model appears to be the more satisfactory since the two separate mechanisms must proceed with the same kinetics to account for the near coincidence of the products. This is considered highly unlikely. Furthermore, the products and kinetics of the reaction are similar to gas-phase acetic anhydride decomposition.

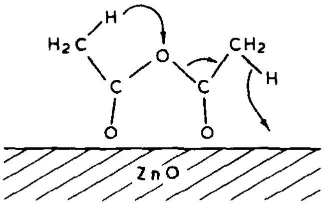

FIG. 3. Schematic diagram of the decomposition of the surface acetic anhydride species by an intramolecular rearrangement. The bidentate nature of the adsorbed species is proposed by analogy with the binding of carboxylates on other surfaces (*6, 7, 21*).

The decomposition of the anhydride species appears to take place in a similar fashion to that of the gas-phase molecule. Hence, initially

$$(CH_3CO)_2O_{(a)} \rightarrow CH_3COOH_{(a)} + CH_2CO_{(a)}, \tag{8}$$

acetic acid and ketene can be produced by an intramolecular rearrangement involving the migration of a hydrogen atom from a methyl group in the molecule to one of the oxygen atoms, and probably the bridging atom as shown in Fig. 3. However, both of these products are probably above their normal desorption temperatures (most molecular absorbates, including acetaldehyde described later, desorb just above room temperature (*1, 2*)) and appear to react further with the surface, as has also been observed on metals (*7, 15, 17*). The major products of this further reaction are CO_2, H_2, and H_2O, which are evolved into the gas phase, and hydrogenated carbon residues, which are left on the surface after the decomposition. The temperature lag of CO_2, H_2O, and acetic acid compared with the ketene is probably due to the relatively strong binding states which can pertain to CO_2 and bidentate carboxylates (*1*) and possibly some forms of hydroxyl groups once they are formed in the steps outlined below. Ketene is a very reactive molecule and appears to interact with oxygen species on the surface (note that excess oxygen is available from step (7)) and CO_2 is produced; a likely mechanism is

$$CH_2CO_{(a)} + O_s \rightarrow CO_{2(a)} + CH_{2(a)}. \tag{9}$$

Further CO_2 is probably produced by acetic acid decomposition, which would occur in the first stage by acetate formation (probably via step (2)) and then by steps (10)–(12) below. These steps have been included for completeness since they take place to a considerable extent on copper (*7*) and silver (*15*) surfaces; it is apparent from Table 1, however, that in the present case of ZnO, step (12) only takes place to a minor extent, whereas large amounts of ketene appear to further react with the surface (much less ketene than acetic acid is evolved).

$$CH_3COO_{(a)} \rightarrow CO_{2(g)} + CH_{3(a)}, \quad (10)$$

$$CH_3COOH_{(a)} \rightarrow CH_3COOH_{(g)}, \quad (11)$$

$$CH_2CO_{(a)} \rightarrow CH_2CO_{(g)}. \quad (12)$$

CO_2 is liberated into the gas phase at 610K (as shown in Fig. 2), as is some of the ketene and most of the acetic acid; hydrogen and water are also liberated in these steps as shown in mechanisms (4), (6), and (14)–(17). The source of the hydrogen for these processes is not likely to be the original acid hydrogens, since these have been postulated to be lost at the lower temperatures and during adsorption. The source of hydrogen, then, must be the methyl groups of the acetate units left on the surface and this occurs via step (2) reoccurring after the rearrangement shown in step (8), thus dissociating acetic acid, and by steps (13a) and (13b) shown below.

$$CH_{2(a)} \rightarrow CH_{x(a)} + (2 - x)H_{(a)}, \quad (13a)$$

$$CH_{3(a)} \rightarrow CH_{x(a)} + (3 - x)H_{(a)}, \quad (13b)$$

$$O_s + H_{(a)} \rightarrow OH_{(a)}, \quad (14)$$

$$OH_{(a)} + H_{(a)} \rightarrow H_2O_{(a)}, \quad (15)$$

$$2H_{(a)} \rightarrow H_{2(g)}, \quad (16)$$

$$H_2O_{(a)} \rightarrow H_2O_{(g)}. \quad (17)$$

The evidence for the further dehydrogenation of the adsorbed methyl and methylene groups is the large amount of hydrogen and water evolution at ~600K and the stoichiometry of the further desorption at 690K, which will now be discussed. This highest-temperature desorption is proposed to be due to the reaction of these surface hydrocarbon residues with surface oxygen, and therefore the carbon : hydrogen ratio gives some idea of the stoichiometry of the $CH_{(x)}$ fragment shown above. It only gives "some idea" because after a complete desorption run it appears that small amounts of carbon were still left on the surface, since gradually, over a series of desorption events, the amount of acetic acid which could be adsorbed decreased. The original amount of adsorption could be restored by oxygen treatment of the sample for 120 min at 600K and 10 Torr pressure and it is likely that carbon was "burned off" the sample in this way. A very similar effect was seen on copper (*7*), silver (*15*), and nickel surfaces (*17*). However, assuming that this amount of carbon was small per experiment, which it appears to have been, then the ratio x has the value of 0.80 ± 0.15 (from an average of six experiments). This then is the upper value of the amount of hydrogen compared with carbon, since the carbon left behind on the surface is not included in the calculation for x. It would appear then that the hydrocarbon residues present above 630K are slightly hydrogen deficient and that a mixture of carbonaceous and partially hydrogenated carbonaceous residues are present on the surface between ~650 and 700K. The final reaction taking place at 700K appears to be oxidation of these residues—excess oxygen probably still remaining from step (7), rather than from lattice oxygen (the zinc oxide having been pretreated in hydrogen to give a reduced surface).

$$CH_x + O_s \rightarrow CO_{(g)} + xH_{(a)}, \quad (18)$$

$$2xH_{(a)} \rightarrow xH_{2(g)}. \quad (19)$$

This last desorption feature presents the major difference observed for acetic acid interaction with the ZnO surface compared with noble metal surfaces (*7, 15*). On these materials all the hydrogen liberated when the acetate starts to decompose is consumed in further reaction, mainly with the $CH_{2(a)}$ and $CH_{3(a)}$ groups, resulting in the absence of any hydrogen desorption coincident with the other products, but evolving a large peak for methane. In the present case, methane desorption is absent and instead

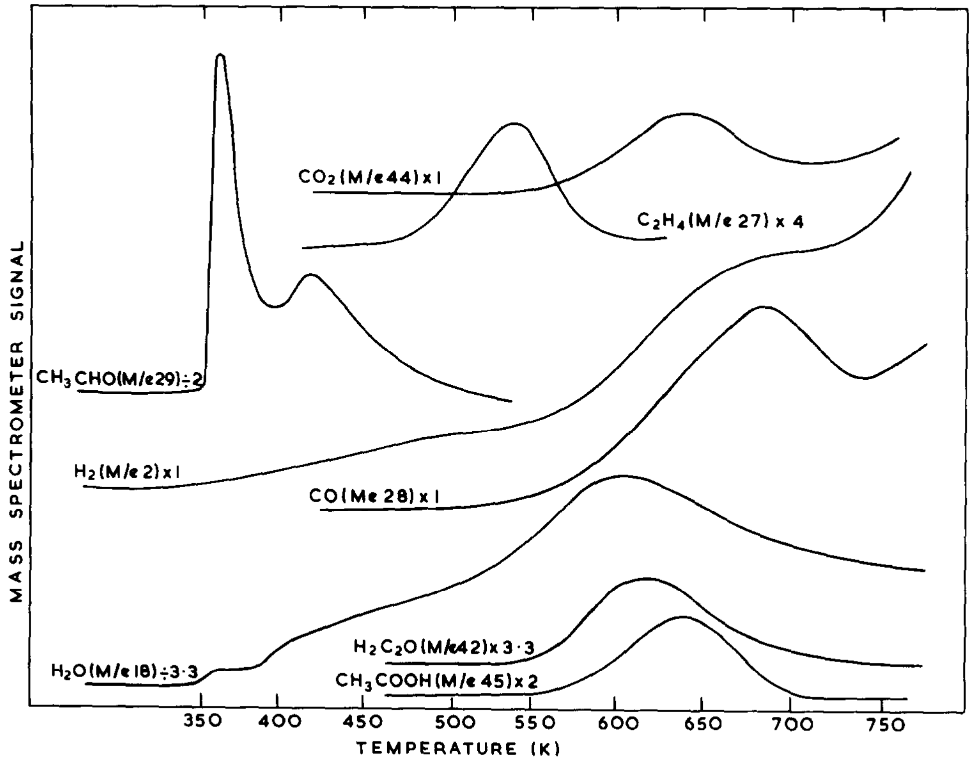

FIG. 4. Temperature-programmed desorption spectrum of products observed after adsorption of acetaldehyde on the ZnO sample at 320K. The different curves are offset for clarity.

the hydrogen either desorbs or reacts with surface oxygen to produce water. All that is left on the surface after the acetate decomposition in the case of the noble metals was carbon (in the case of Ag, approximately 2% of the carbon initially adsorbed on the surface in the acetic acid was left behind (*15*)), whereas in this case these species were partially hydrogenated and stabilized by the surface—probably by interaction with lattice oxygen atoms.

A further interesting similarity between the acetate decomposition on Ag and on ZnO is that the ketene appears slightly lower in temperature than those for the other peaks (by approximately 20K in the present case and ~40K for the Ag (110) system (*15*)). This indicates that the acetic acid product of step (8) is held considerably more strongly than the ketene, which desorbs immediately (at least, that amount which does not further react with the surface), and subsequent interaction with the oxygen atoms of the surface results in a lag of product evolution into the gas phase. (It must be noted that this effect was not observed on copper, where all the products desorbed coincidently (*7*).)

The Adsorption of Acetaldehyde

Figure 4 shows the temperature-programmed desorption spectrum obtained after acetaldehyde adsorption on the hydrogen pretreated zinc oxide surface at 320K. The products desorbed are very similar to those from acetic acid adsorption, except that large amounts of acetaldehyde are desorbed in the 300–450K region. In this case the CO, H_2 peak seen at 690K for acetic acid adsorption is less well resolved since in this series of experiments a much more steeply rising background pressure was present (due to desorption from supports and the walls of the vessel). A further major difference between acetaldehyde and acetic acid experiments is that the former shows the desorption of ethylene at ~530K as evidenced by large m/e 28, 27, and 26 evolution in that temperature region. The total coverage by acetaldehyde and by the various intermediates on the surface is given in Table 1.

In this case a large amount of acetaldehyde appears to be adsorbed in a molecular form on the surface and desorbs intact again in the low-temperature region (step (23)). Adsorption can be represented by

$$CH_3CHO_{(g)} \rightarrow CH_3CHO_{(a)}. \qquad (20)$$

It is clear, however, that some of the adsorbed molecules also react with the surface since the same products seen for acetic acid are observed to desorb above 600K, thus the acetate is formed by interaction of acetaldehyde with surface oxygen species:

$$CH_3CHO_{(a)} + O_{(s)} \rightarrow CH_3CHOO_{(a)}, \qquad (21)$$

$$CH_3CHOO_{(a)} \rightarrow CH_3COO_{(a)} + H_{(a)}. \qquad (22)$$

This is completely analogous to the reactions observed in the previous work (*1*) for formaldehyde interaction with the ZnO surface. In that case the formate was formed. In a similar way the acetate is formed here by nucleophilic attack at the carbonyl group by the highly electronegative surface oxygen atom. This results in the formation of the hydrogenated acetate species, which was shown to be unstable on the surface of Ag(110) above 250K (*15*), and so rapidly decomposes at room temperature via a dehydrogenation mechanism, step (22) (as confirmed on the Ag(110) plane). Thus at the low temperatures some water is liberated and unreacted acetaldehyde also desorbs:

$$H_{(a)} + O_{(s)} \rightarrow OH_{(a)}, \qquad (14)$$

$$H_{(a)} + OH_{(a)} \rightarrow H_2O_{(a)}, \qquad (15)$$

$$H_2O_{(a)} \rightarrow H_2O_{(g)}, \qquad (17)$$

$$CH_3CHO_{(a)} \rightarrow CH_3CHO_{(g)}. \qquad (23)$$

In addition to the adsorbed acetate species a further intermediate is also present on the surface at this stage, as evidenced by the ethylene desorption seen at 530K. This intermediate is most likely to be the ethoxy species, since ethanol adsorption on this surface was found to produce the same desorption feature at that temperature (*2*). The simplest route to ethoxy production is by acetaldehyde hydrogenation as shown below, the hydrogen for this reaction,

$$CH_3CHO_{(a)} + H_{(a)} \rightarrow CH_3CH_2O_{(a)}, \qquad (24)$$

being supplied by step (22). It is likely that steps (21)–(23), and (24) have all occurred at room temperature. This last reaction is in complete contrast to that observed on metal surfaces. First, no evidence was found for ethoxy formation on copper (*7*) or silver surfaces (*15*) after the adsorption of acetaldehyde on the oxygen-predosed metals. Second, the ethoxy species on the noble metals (produced from ethanol oxidation) decomposes to yield acetaldehyde in the gas phase, not ethylene as is the case here, that is, the metals subtend further dehydrogenation whereas the ZnO surface subtends dehydration of the ethoxy. As proposed by Bowker *et al.* (*2*), the ethoxy appears to interact further with the ZnO surface primarily through the β carbon atom, whereas on the metals the αC–H is split. Thus on ZnO,

$$O_{(s)} + CH_3CH_2O_{(a)} \rightarrow CH_2CH_2O_{(a)} + OH_{(a)}, \qquad (25)$$

$$CH_2CH_2O_{(a)} \rightarrow CH_2CH_{2(g)} + O_{(s)}, \qquad (26)$$

$$2OH_{(a)} \rightarrow H_2O_{(g)} + O_{(s)}, \qquad (27)$$

however, in the previous work only hydrogen, and not water, was desorbed from ethoxy decomposition (*2*). In the present work Fig. 4 shows no distinct H_2 peak and water may be evolved coincidently with the ethylene, but since the water desorption in total is much bigger than the ethylene (its scale is of much lower sensitivity) the peak may well be submerged. Suffice it to say that large amounts of water are being desorbed from the surface at the same time as ethylene.

All that remains on the surface after this reaction, then, are the acetate groupings and possibly some surplus oxygen atoms. Indeed, relatively more water than hydrogen is evolved in this case, seemingly confirming the latter point. These acetates appear to decompose in a very similar fashion to those from acetic acid described above, although the coverage appears to be quite a lot lower and the acetate products appear approximately 30K higher in temperature. The latter two facts are probably related—if the rate-limiting step in the acetate decomposition is the reaction between two acetate groupings then such a second-order process would result in a coverage dependence of the product peaks in just the way indicated. However, arguments against a second-order process will be invoked below and so other possibilities must also be considered. In particular, the strength of binding of oxygen atoms to the zinc oxide surface has been shown to be strongly dependent on the number of defects present on the surface, and the more defects, the stronger the binding energy and the harder it becomes to remove oxygen (*19*, *20*). So, perhaps in this case too, compared with the higher acetate coverage from acetic acid, the total apparent oxygen coverage of the surface is lower and thus the acetates are bound more strongly. Once again carbonaceous residues are left after acetate decomposition and then decompose by reaction with surface oxygen to CO and H_2 in the gas phase at ~680K.

STABILITY OF THE ACETATE/ANHYDRIDE ON DIFFERENT SURFACES

Results for the stability of acetate and anhydride on various surfaces obtained in this work and others are presented in a comparative way in Table 2. The most interesting feature of this compilation is the similarity of the stability of these species on the zinc oxide and noble metal surfaces; the nickel surface is in contrast to this, exhibiting an anhydride intermediate but of relatively low stability. To give reasonable comparative values for decomposition activation energies, values were determined using Eq. (A) given in the Introduction and an assumed normal preexponential factor of 10^{13} s^{-1}, since the lineshapes of some of the desorption patterns are not amenable to the usual analysis methods; this is due to lineshape broadening in the case of ZnO (due to readsorption within the powder sample), while in the case of Ag(110) the desorption envelope appeared to comprise at least two sets of overlapping peaks (*15*). In the case of Cu and Ni, however, it must be noted that lineshape analysis was carried

TABLE 2

Acetate/Anhydride Stabilities for Various Surfaces

Surface	Peak temperature/ heating rate (K s^{-1})	Decomposition[a] activation energy (kJ $mole^{-1}$)	Normalized[b] peak temperature (K)	Reference
ZnO (polycrystalline)	600K/0.7	165	608	Present work
Ag(110)	650K/25	161	590	(*15*)
Cu(110)	590K/4	155	568	(*7*)
Ni(110)	440K/9	111	412	(*17*)

[a] Calculated from Eq. (A) assuming a frequency factor for desorption of 10^{13} s^{-1}.

[b] Calculated for a heating rate of 1K s^{-1}.

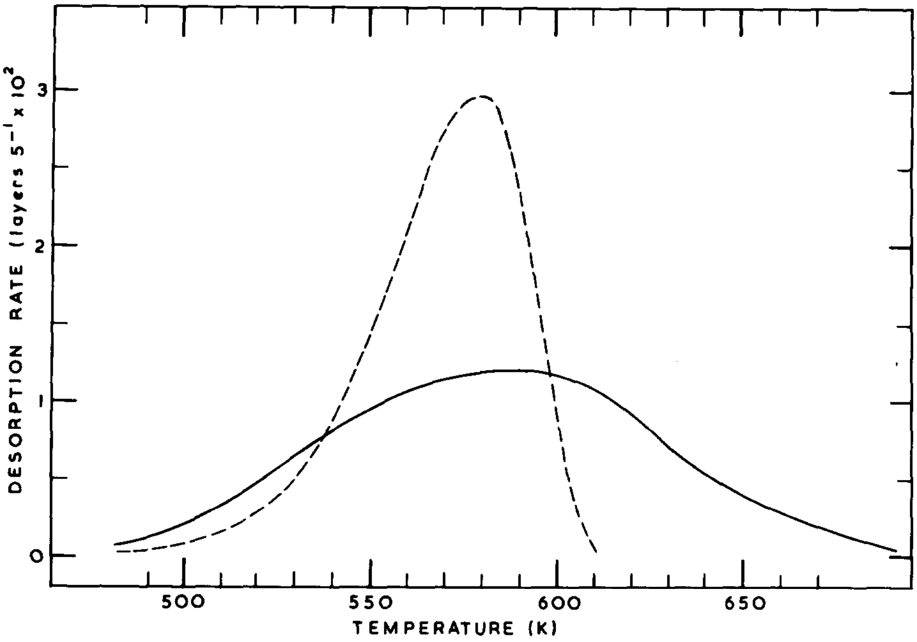

FIG. 5. Comparison of the experimentally observed desorption curve for ketene (——) with theoretical lineshape (---) which would be expected for desorption (with no readsorption effects) if the surface process occurred with kinetics identical to those of the gas-phase acetic anhydride decomposition process (*16*).

out and showed preexponential factors higher than normal, and in the case of Ni the kinetics were complex, showing an autocatalytic decomposition mechanism and resulting in very low peak widths (*17*). Nonetheless, it is felt that the form of presentation in Table 2 gives a useful basis for discussion.

The similar stability of the acetate/anhydride species on ZnO, Cu, and Ag is rather surprising since the single carbon analog is the formate and this shows considerable differences in stability between the three surfaces. Thus on Ag(110) the formate decomposition peak is at 410K (heating rate 17K s^{-1}) (*21*) and on Cu(110) the peak is at 470K (heating rate 4K s^{-1}) (*6*), while the formate is most stable on ZnO, giving a peak rate at 570K (heating rate 0.7K s^{-1}) (*1*). Clearly, then, for the formate these materials subtend considerably different activity, as should be expected since these are indeed materials of very different adsorption properties. An explanation for the similarity of stabilities of the acetate/anhydrides is possibly that, rather than the decomposition reaction being dominated by the breakage of bonds which are interacting with the surface, the breakup is determined by the intramolecular rearrangements of atoms occurring ~3 Å away from the surface plane (see Fig. 3). The decomposition rate is then determined by kinetics similar to those in the gas phase and is less influenced by the surface involved. To illustrate this point further Fig. 5 shows two curves, one for the ketene evolution also shown in Fig. 2, which is assumed to give the best measure of the anhydride decomposition rate on the ZnO surface, and the second is a desorption curve which would be expected if the desorption rate followed the gas-phase kinetics exactly. The rate constant for the latter is given by Blake and Speis (*16*) as

$$k = 10^{11.27}\ \mathrm{s}^{-1} \exp(-137.4\ \mathrm{kJ\ mole}^{-1}/RT) \tag{28}$$

and so the desorption rate (assuming no lateral interaction effects on the decomposition energy) becomes

$$d\theta/dt = k\theta \qquad (29)$$

or, in terms of temperature units, $\beta = dT/dt$ and so

$$d\theta/dT = k\theta/\beta, \qquad (30)$$

where β is the heating rate (in the present case 0.7K s^{-1}). The curve generated from these relations is shown in Fig. 5 and, for simplicity, it is assumed that the saturation coverage corresponds to $\theta = 1$, and in turn the same is assumed for the experimental curve (that is, $\theta = 1 = 4.7 \times 10^{14}$ acetates cm^{-2}). The theoretical lineshape is typically first order with the integral above the peak maximum temperature being less than that below it. The experimental curve, however, is more distorted toward higher temperatures, the result of broadening due to the powdered nature of the sample and occurrence of multiple collisions within the catalyst, and even possible readsorption/desorption events (*22*). Nevertheless, since the temperature range of desorption and the peak temperature for the two curves are very similar, it is clear that the decomposition kinetics on the surface are close to those in the gas phase, indicating that step (8) may well be the rate-determining step in decomposition. Thus the process is first order and the shift in peak position for the acetate in Figs. 2 and 4 cannot be postulated to be due to the coverage dependence of second-order peak positions (first-order desorption processes, with coverage-independent kinetic parameters, show an invariant peak maximum temperature for different coverages of adsorbate).

It is evident from Table 2 that the nickel surface (and probably other metals in the transition series with unfilled *d*-bands) is much more active toward decomposition of the anhydride entity, and since decomposition occurs at a temperature far below the range indicated in Fig. 5, it is reasonable to assert that the rate-determining step involves the surface in the transition state. The stronger influence of the surface in this case is also manifested by the product pattern, which is completely different from that observed for the other three materials listed in Table 2. Thus the only major products are CO, CO_2, and H_2 and the carbon bonds are completely dehydrogenated in the decomposition process (*17*). Seemingly then, the milder catalytic properties of the noble metals and of ZnO prove more efficacious for the dehydration of acetic acid to ketene.

CONCLUSIONS

Acetic acid and acetaldehyde were shown to adsorb and react with the ZnO surface to produce a strongly bound acetate species. The decomposition of the acetate occurs in a complex fashion to yield major products of ketene, acetic acid, carbon dioxide, hydrogen, and water. It is shown that, as proposed for noble metal surfaces by Madix *et al.* (*7, 15*), an acetic anhydride intermediate is produced by reaction between two acetates and that this dominates the decomposition process. Indeed, the temperature of decomposition is very similar on ZnO and the noble metals and is postulated to be controlled by a process not strongly influenced by the surface, that is, an intramolecular hydrogen transfer within the anhydride moiety. In the case of acetaldehyde adsorption an additional hydrogenation reaction takes place to produce an ethoxy intermediate which decomposes to liberate ethylene into the gas phase.

REFERENCES

1. Bowker, M., Houghton, H., and Waugh, K. C., *J. Chem. Soc. Faraday I* **77**, 3023 (1981).
2. Bowker, M., Houghton, H., and Waugh, K. C., *J. Chem. Soc. Faraday I* **78**, 2573 (1982).
3. See, for example, Madix, R. J., *Advan. Catal.* **29**, 1 (1981).
4. Bowker, M., and Madix, R. J., *Surf. Sci.* **95**, 190 (1980); *Surf. Sci.* **116**, 549 (1982).
5. Benziger, J., Ko, E. I., and Madix, R. J., *J. Catal.* **58**, 149 (1979).
6. Bowker, M., and Madix, R. J., *Surf. Sci.* **102**, 542 (1981).

7. Bowker, M., and Madix, R. J., *Appl. Surf. Sci.* **8,** 299 (1981).
8. Parrott, S., Rogers, J. W., and White, J. M., *Appl. Surf. Sci.* **1,** 443 (1978).
9. Falconer, J. L., and Madix, R. J., *J. Catal.* **48,** 262 (1977).
10. Benziger, J., Ko, E., and Madix, R. J., *J. Catal.* **54,** 414 (1978).
11. Luth, H., Rubloff, G. W., and Grobman, W. D., *Surf. Sci.* **63,** 325 (1977).
12. Rubloff, G. W., Grobman, W. D., and Luth, H., *Phys. Rev. B* **14,** 1450 (1976).
13. Ueno, A., Onishi, T., and Tamaru, K., *Trans. Faraday Soc.* **67,** 3585 (1971).
14. Rubloff, G. W., Luth, H., and Grobman, W. D., *Chem. Phys. Lett.* **39,** 493 (1976).
15. Barteau, M., Bowker, M., and Madix, R. J., *J. Catal.* **67,** 118 (1981).
16. Blake, P., and Speis, A., *J. Chem. Soc. B,* 1877 (1971).
17. Madix, R. J., Falconer, J. L., and Suszko, A. M., *Surf. Sci.* **54,** 6 (1976).
18. Kishi, K., and Ikeda, S., *Appl. Surf. Sci.* **5,** 7 (1980).
19. Green, M., and Lauks, I. R., *J. Chem. Soc. Faraday II* **74,** 2724 (1978).
20. Gopel, W., *Surf. Sci.* **62,** 165 (1977).
21. Barteau, M., Bowker, M., and Madix, R. J., *Surf. Sci.* **94,** 303 (1980).
22. See, for example, Konvalinka, J., Scholten, J., and Rasser, J. C., *J. Catal.* **48,** 365 (1977).